Supplemental Figures: Genome-wide nucleosome and transcription factor responses to genetic perturbations reveal chromatin-mediated mechanisms of transcriptional regulation

Kevin Moyung[1,2], Yulong Li[2,3,†], Heather K. MacAlpine[2],

Alexander J. Hartemink[1,3,*], and David M. MacAlpine[1,2,*]

[1] Program in Computational Biology and Bioinformatics, Duke University, Durham, NC 27708

[2] Department of Pharmacology and Cancer Biology, Duke University Medical Center, Durham, NC 27710

[3] Department of Computer Science, Duke University, Durham, NC 27708

[†] Current affiliation: Jiangsu Raman Medical Equipment Co., Ltd., Taizhou 225300, Jiangsu, China

* To whom correspondence should be addressed

Email: david.macalpine@duke.edu

Phone: +1 919-450-8995

Email: amink@cs.duke.edu

Phone: +1 919-660-6514

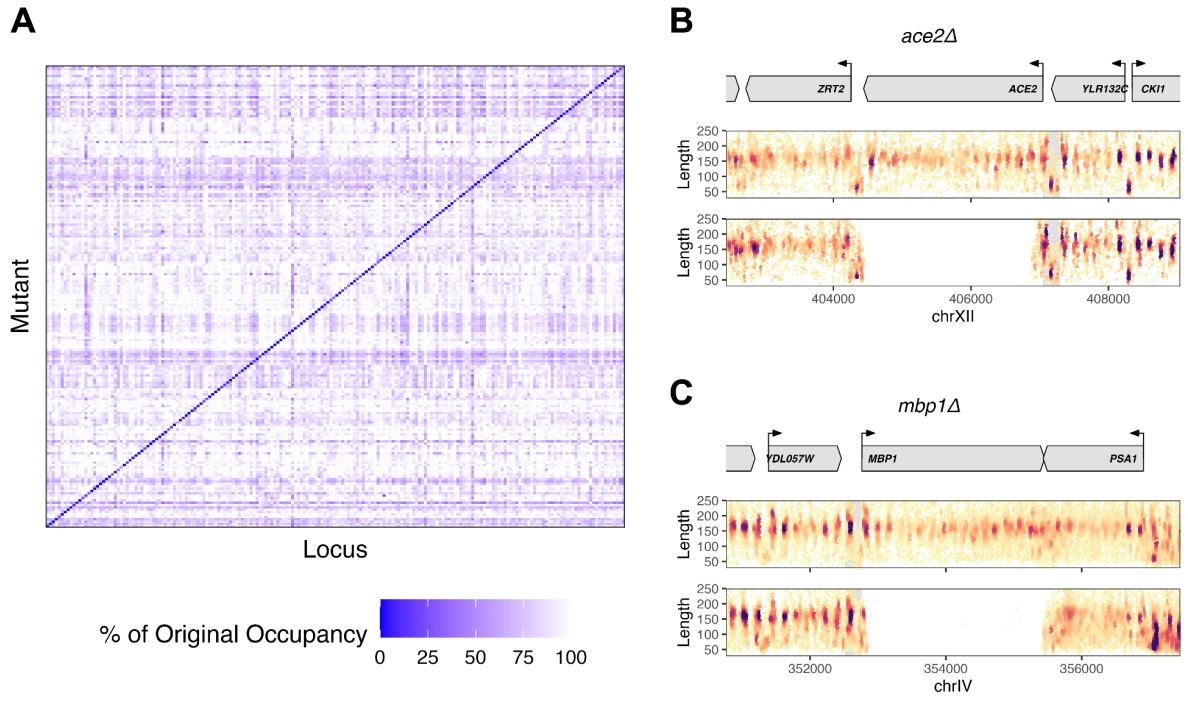

Supplemental Figure S1

Validation of the deletion mutants used in this study. (A) Heatmap displaying the percent of nucleosome occupancy relative to the control in each mutant at each mutant gene locus. The diagonal represents a significant dropout in chromatin occupancy, indicating a precise deletion at the ORF of every mutant. **(B)** Plot of MNase-seq reads for *ace2*Δ showing the absence of reads in the *ACE2* locus. **(C)** Plot of MNase-seq reads for *mbp1*Δ showing the absence of reads in the *MBP1* locus.

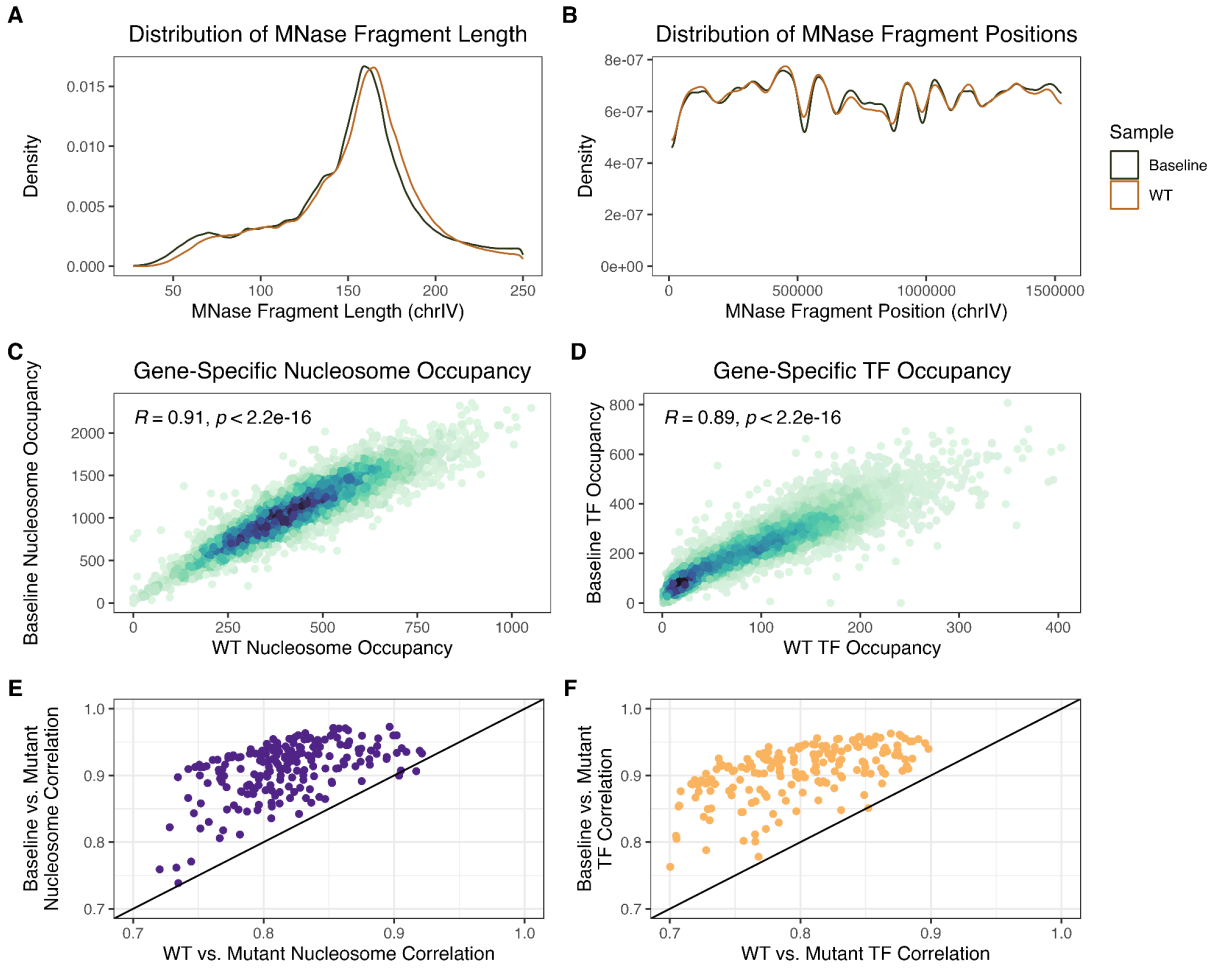

Supplemental Figure S2

Wild-type (WT) yeast sample compared to the baseline control, which is computed from all 201 mutant MNase-seq samples. (A) Distribution of MNase fragment lengths between the baseline control and WT on chromosome IV. **(B)** Distribution of MNase fragment midpoint positions between the baseline control and WT on chromosome IV. **(C)** Comparison of nucleosome-sized fragments (140–180 bp) in gene bodies between baseline control and WT. **(D)** Comparison of TF-sized fragments (40–100 bp) in gene promoters between baseline control and WT. Comparison scatter plots across all mutants of **(E)** nucleosome and **(F)** TF occupancies between the baseline control used in the study and the WT sample. Points above the diagonal indicate a higher correlation in the baseline control, and points below the diagonal indicate a higher correlation in the individual WT sample.

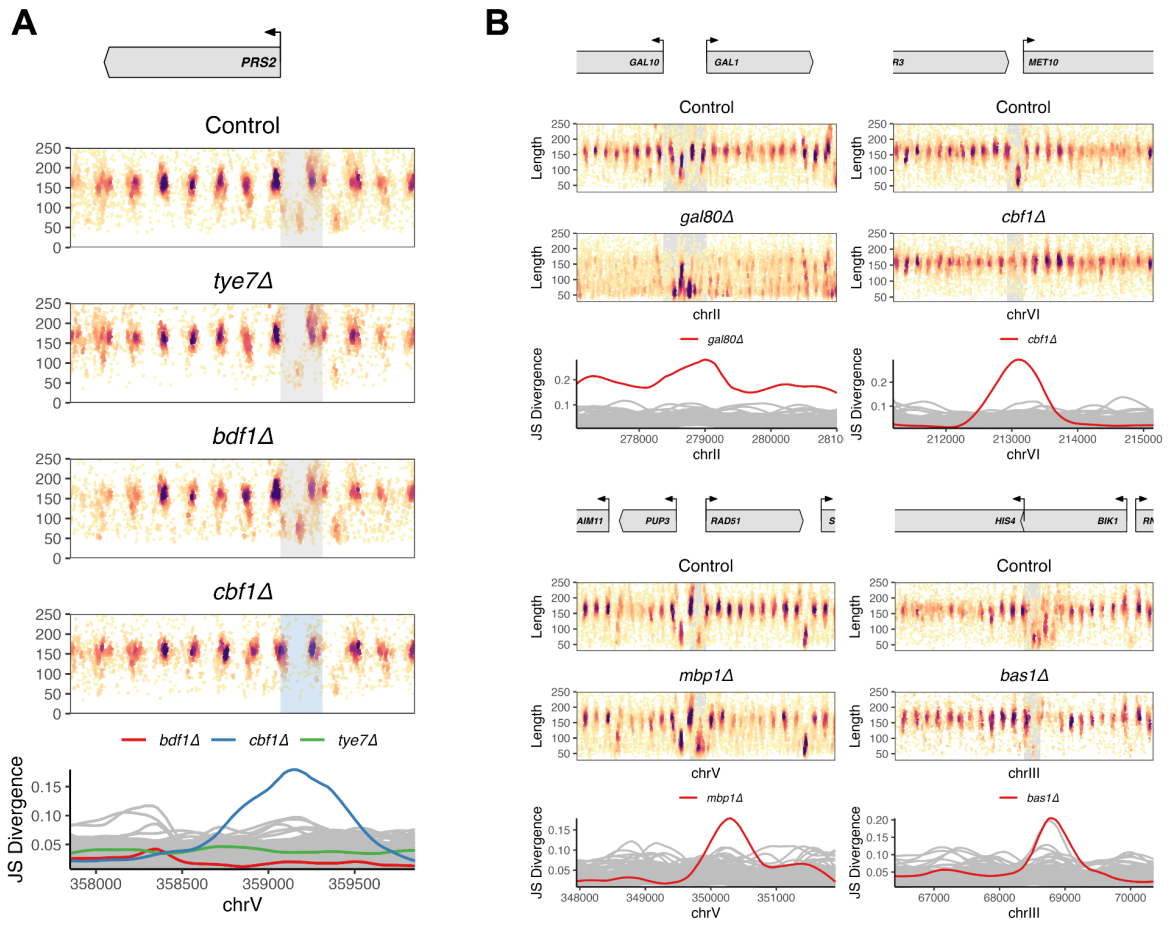

Supplemental Figure S3

Benchmarking the JS divergence measure in known mutant-gene regulatory interactions. (A) The PRS2 promoter contains Tye7, Bdf1, and Cbf1 binding sites. The deletion of CBF1 (*cbf1Δ*, blue line), causes a significant chromatin change represented by the peak in JS divergence, whereas tye7Δ (green), bdf1Δ (red), and other mutants (gray) do not result in notable changes to the chromatin at this locus. **(B)** Known regulation at multiple promoters (GAL1-10, MET10, RAD51, and HIS4) showing elevated JS divergences (red) compared to other mutants (gray).

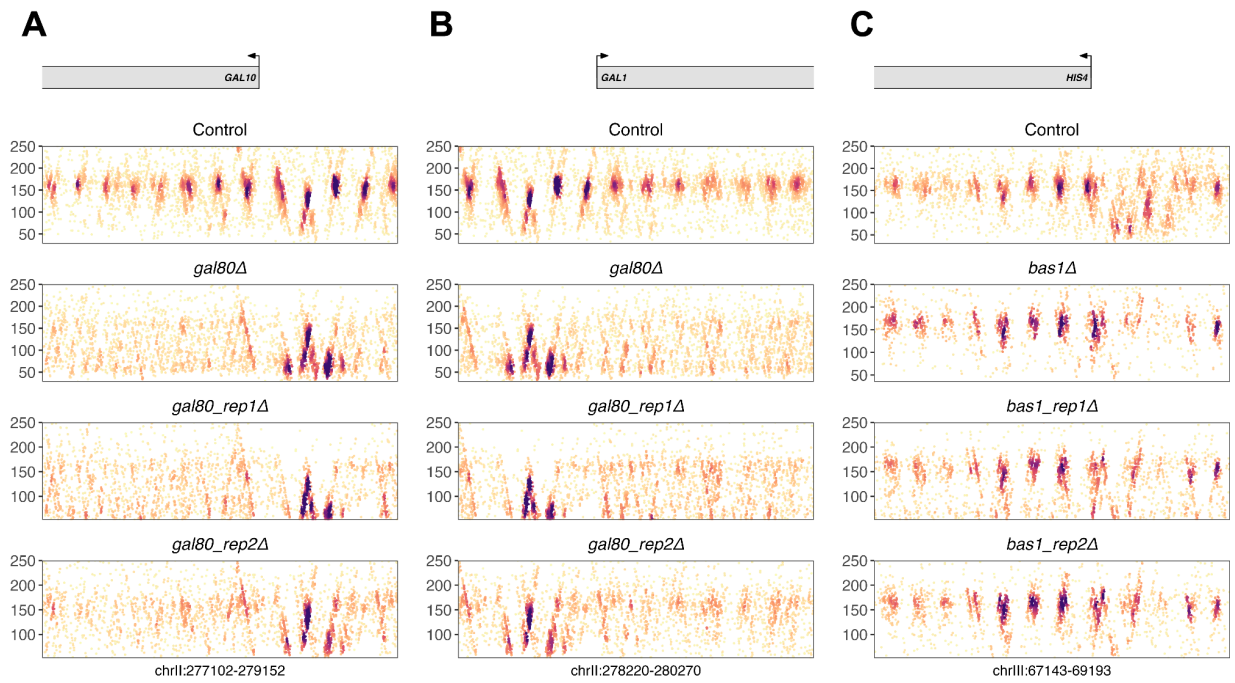

Supplemental Figure S4

MNase fragment plots of mutants at key loci compared to their replicates. *gal80*Δ compared to two *gal80*Δ replicates at the **(A)** *GAL10* locus and **(B)** *GAL1* locus. **(C)** *bas1*Δ compared to two *bas1*Δ replicates at the HIS4 locus.

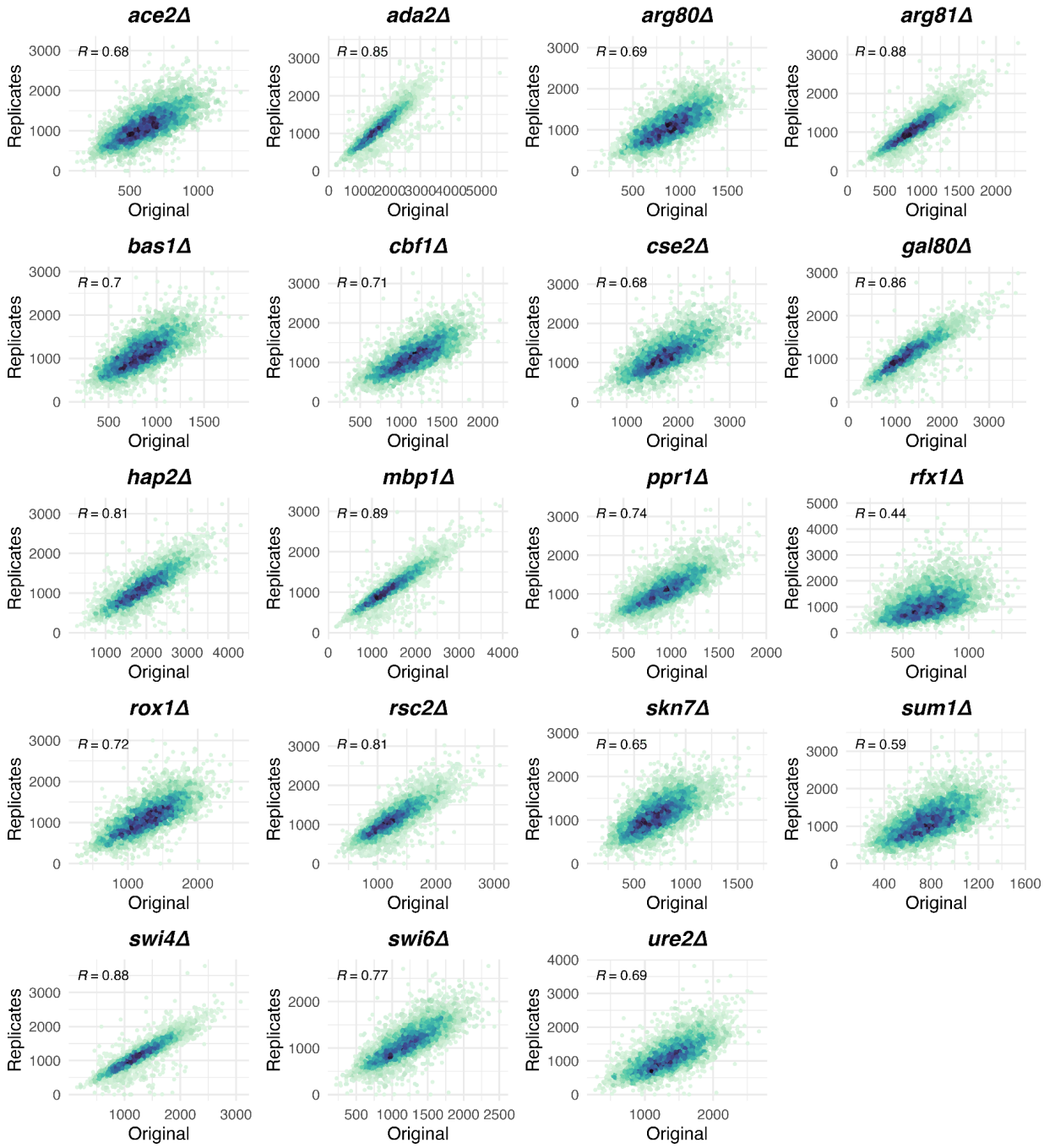

Supplemental Figure S5

Validation of select mutants using two additional replicates. A set of 19 mutants were selected and two additional biological replicates of MNase-seq were generated for each mutant. Each scatter plot represents the nucleosome-sized MNase fragments at a gene between merged replicate mutants (y-axis) vs. the original mutant (x-axis), with every point representing a gene/locus. R values are Pearson correlations.

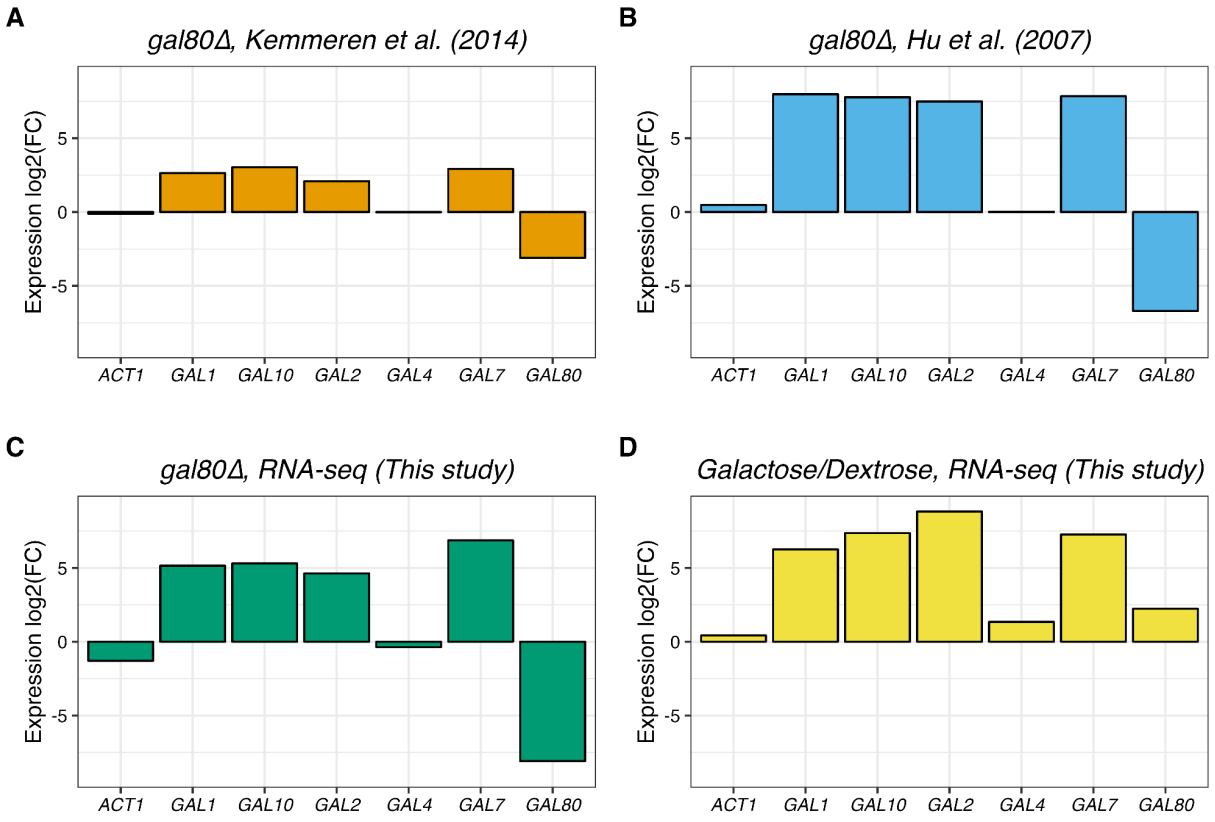

Supplemental Figure S6

Impact of *GAL80* deletion (*gal80*Δ) on gene expression at various *GAL* loci. Values are reported as $\log_2$ fold change in gene expression. The housekeeping gene actin, *ACT1*, is included as a control. **(A)** Microarray expression data for *gal80*Δ from Kemmeren et al. (2014). **(B)** Microarray expression data for *gal80*Δ from Hu et al. (2007). **(C)** RNA-seq data in this study for *gal80*Δ. (A), (B), and (C) were all performed in rich media containing 2% dextrose. **(D)** RNA-seq data in this study for wild-type yeast strains grown in galactose compared to dextrose.

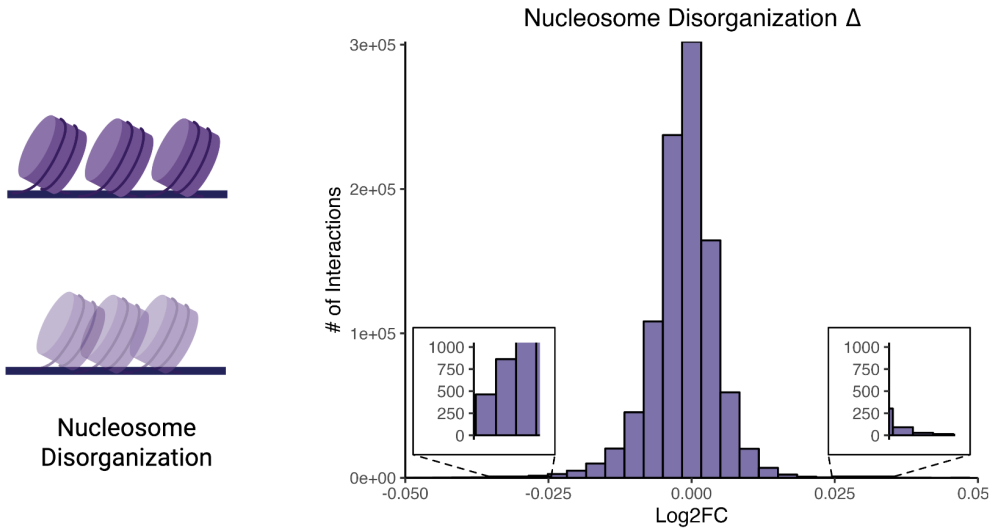

Supplemental Figure S7

Nucleosome disorganization changes across all captured mutant-gene interactions. Inset plots highlight the interactions with the lowest and highest nucleosome disorganization changes, respectively. Positive values indicate an increase in nucleosome disorganization, and negative values indicate a decrease in nucleosome disorganization.

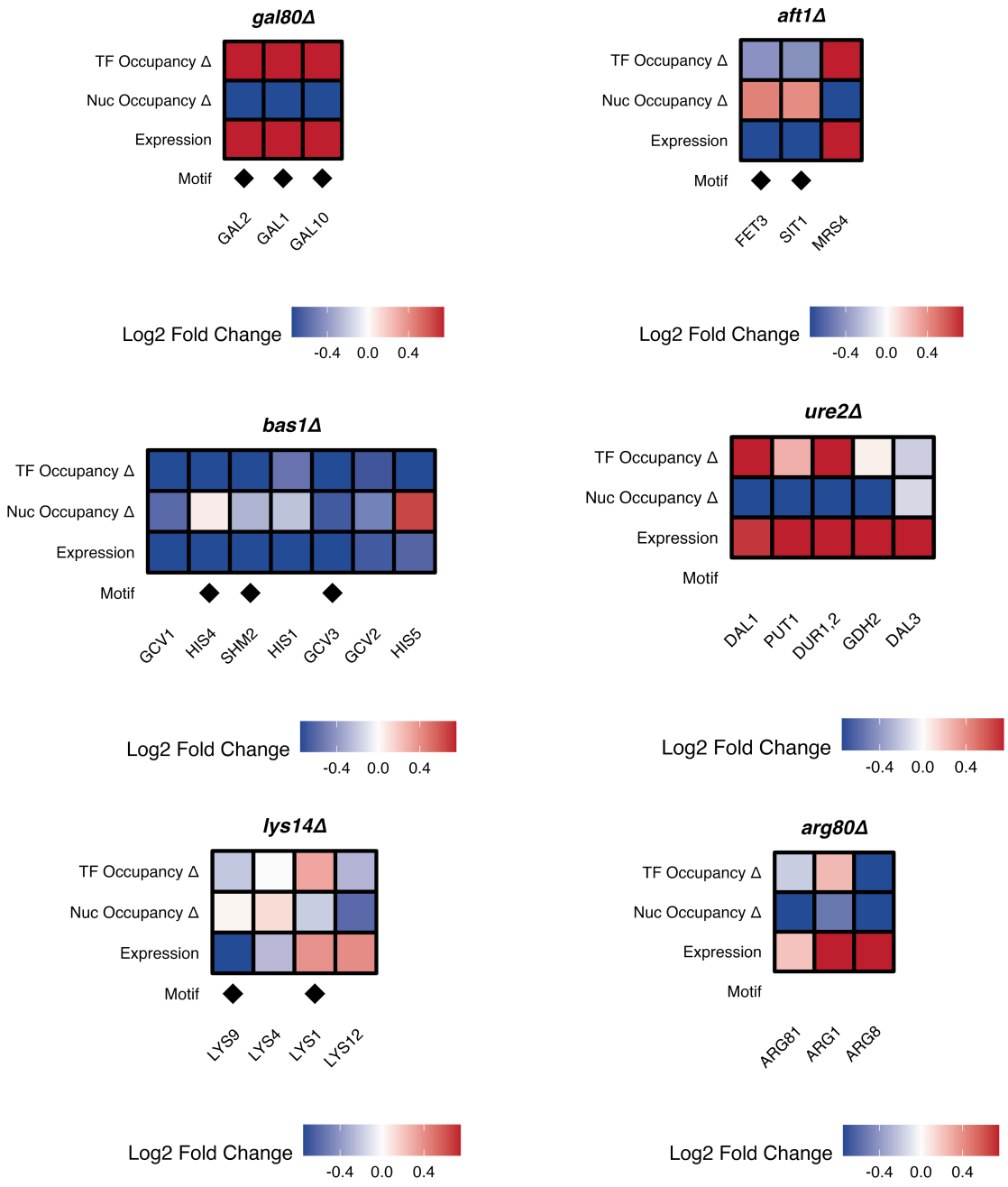

Supplemental Figure S8

Genes in annotated pathways contain chromatin changes associated with the deletion of specific TFs. The heatmaps display nucleosome and TF occupancy changes, along with gene expression changes ($\log_2$(FC)). A gene is annotated with a black diamond if a binding motif for the deleted factor is present in its promoter.

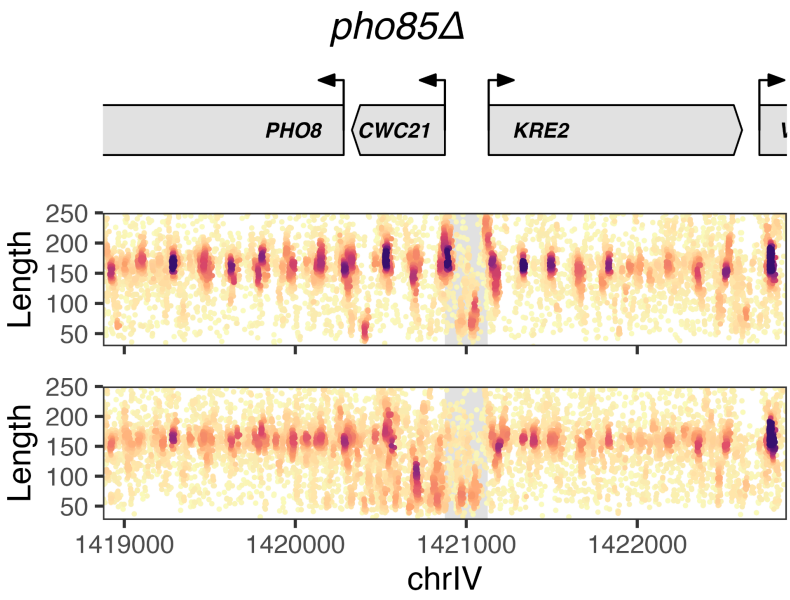

Supplemental Figure S9

Observed chromatin changes sometimes extend to neighboring genes. Deletion of *PHO85* (*pho85Δ*) resulted in chromatin and expression changes at *PHO8,* but also resulted in chromatin changes at *CWC21* and *KRE2*; the latter two genes were not associated with strong gene expression changes, however.

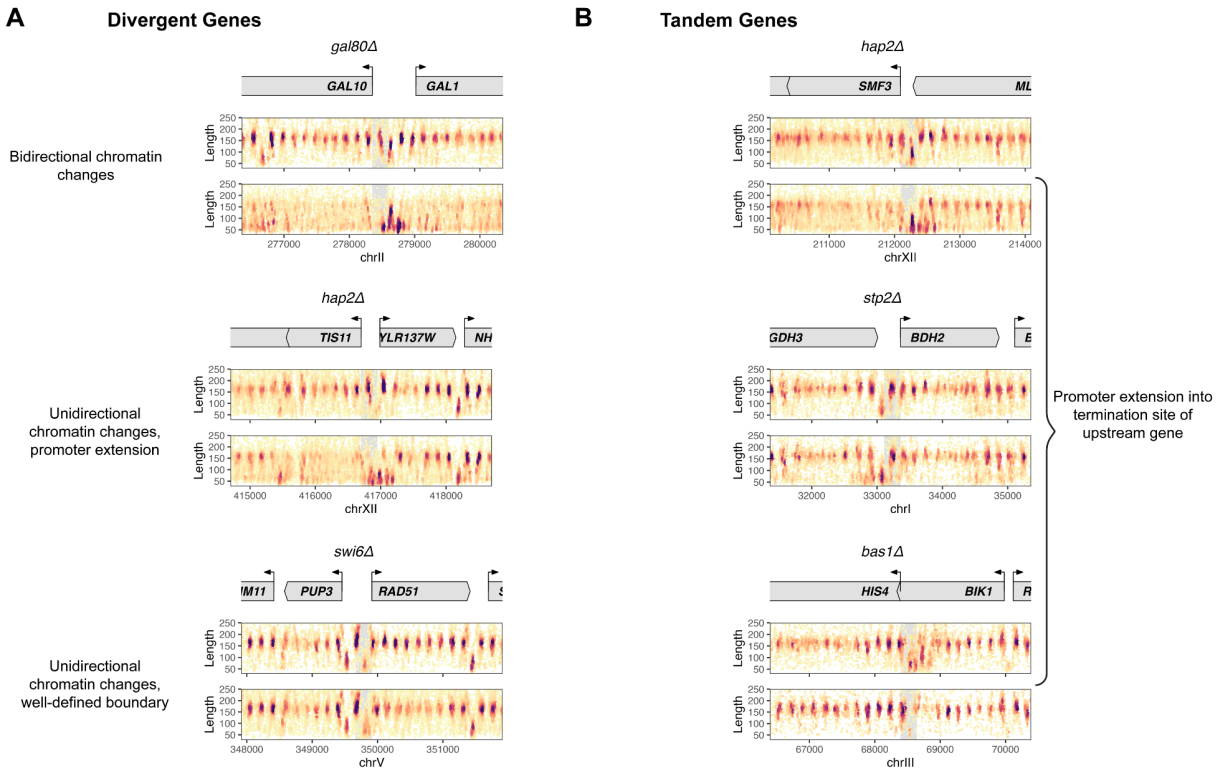

Supplemental Figure S10

Potential modes of transcriptional regulation and interference in neighboring genes revealed by chromatin changes. (A) In divergent genes, 3 distinct modes of chromatin changes are observed at shared promoters. The shared promoter can exhibit bidirectional chromatin changes, unidirectional (single gene) chromatin changes with promoter activity extending into the neighboring (inactive) gene, or unidirectional chromatin changes with a well-defined boundary despite the close proximity. **(B)** In tandem genes, we observed cases where the promoter of an upregulated gene extends well into the polyadenylation site (PAS) of its neighboring upstream gene, when the upstream gene is itself inactive (based on the data of Kemmeren et al.).

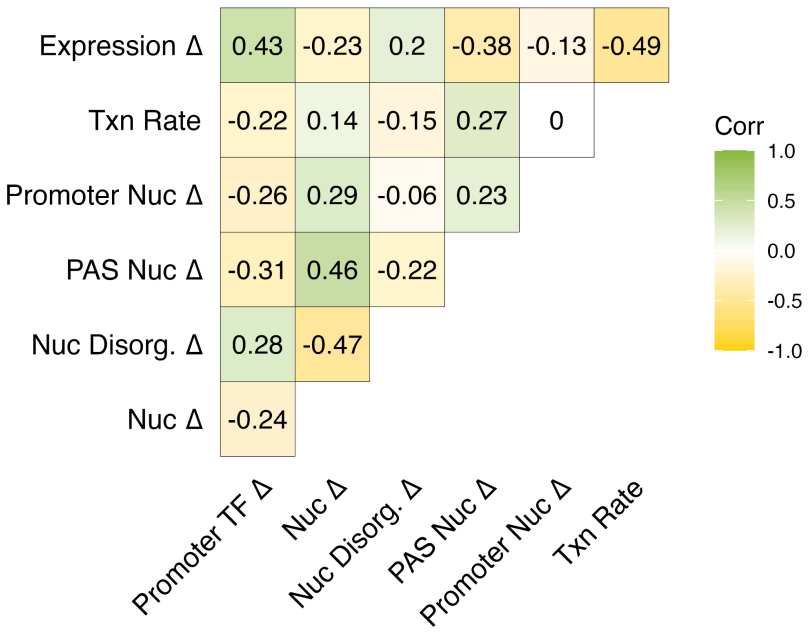

Supplemental Figure S11

Heatmap displaying Pearson correlations between key chromatin features, gene expression, and transcription rate. Changes in chromatin features are calculated from MNase data reported in this study. Changes in gene expression are calculated from Kemmeren et al. (2014). Transcription rates are determined by NET-seq, as reported by Churchman and Weissman (2011).

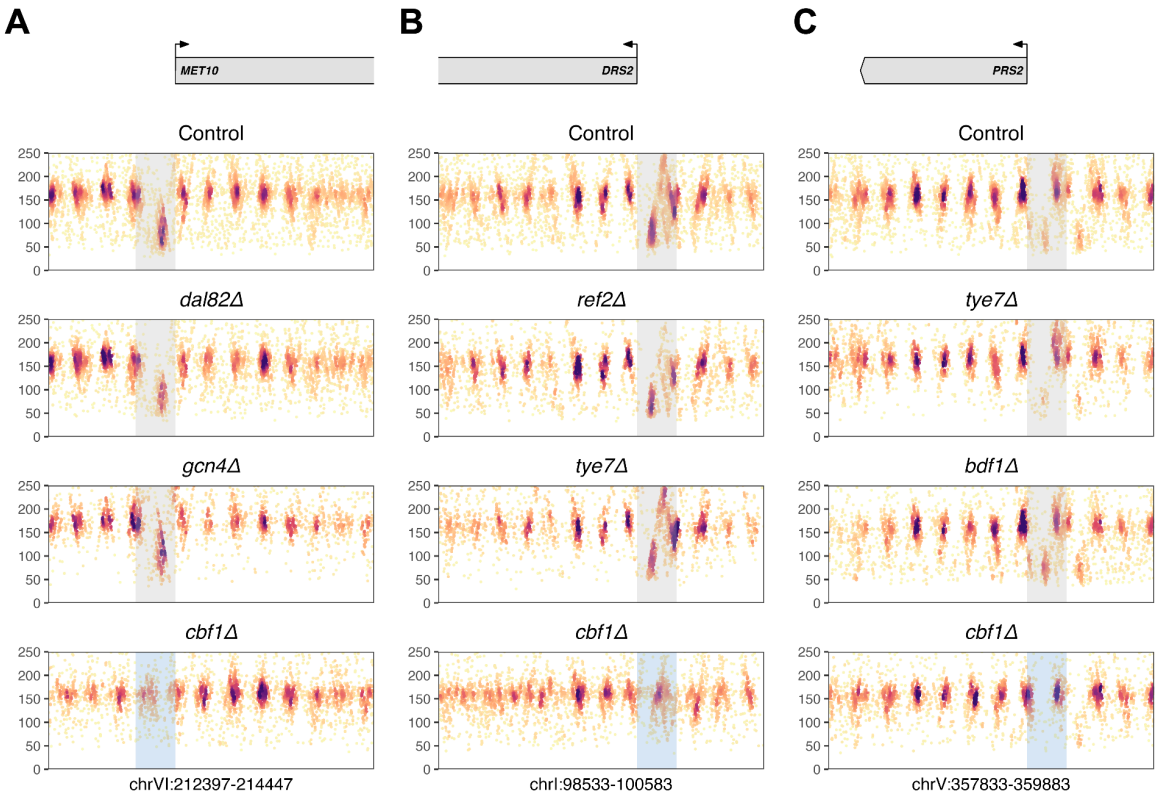

Supplemental Figure S12

Pioneering characteristics of Cbf1 observed at multiple promoters. The promoters of *MET10*, *DRS2*, and *PRS2* contain binding sites for multiple TFs in our dataset. However, only the deletion of *CBF1* (*cbf1Δ)* resulted in significant TF occupancy changes compared to the other TF deletion mutants.

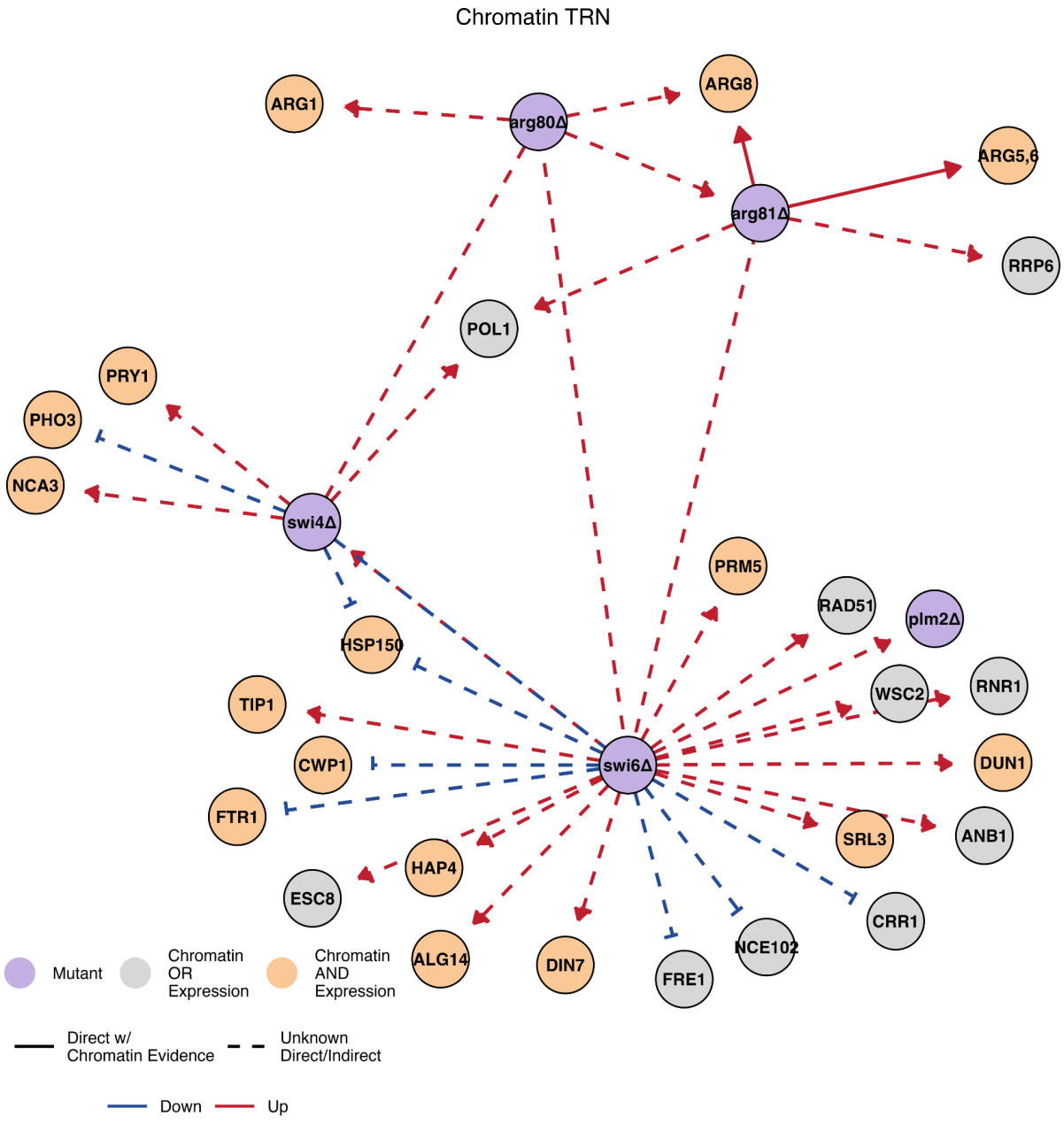

Supplemental Figure S13

Changes in chromatin structure can recapitulate shared regulatory networks between more than one mutant. *arg80Δ/arg81Δ* share overlapping targets as observed from chromatin changes, as well as *swi4Δ/swi6Δ*.

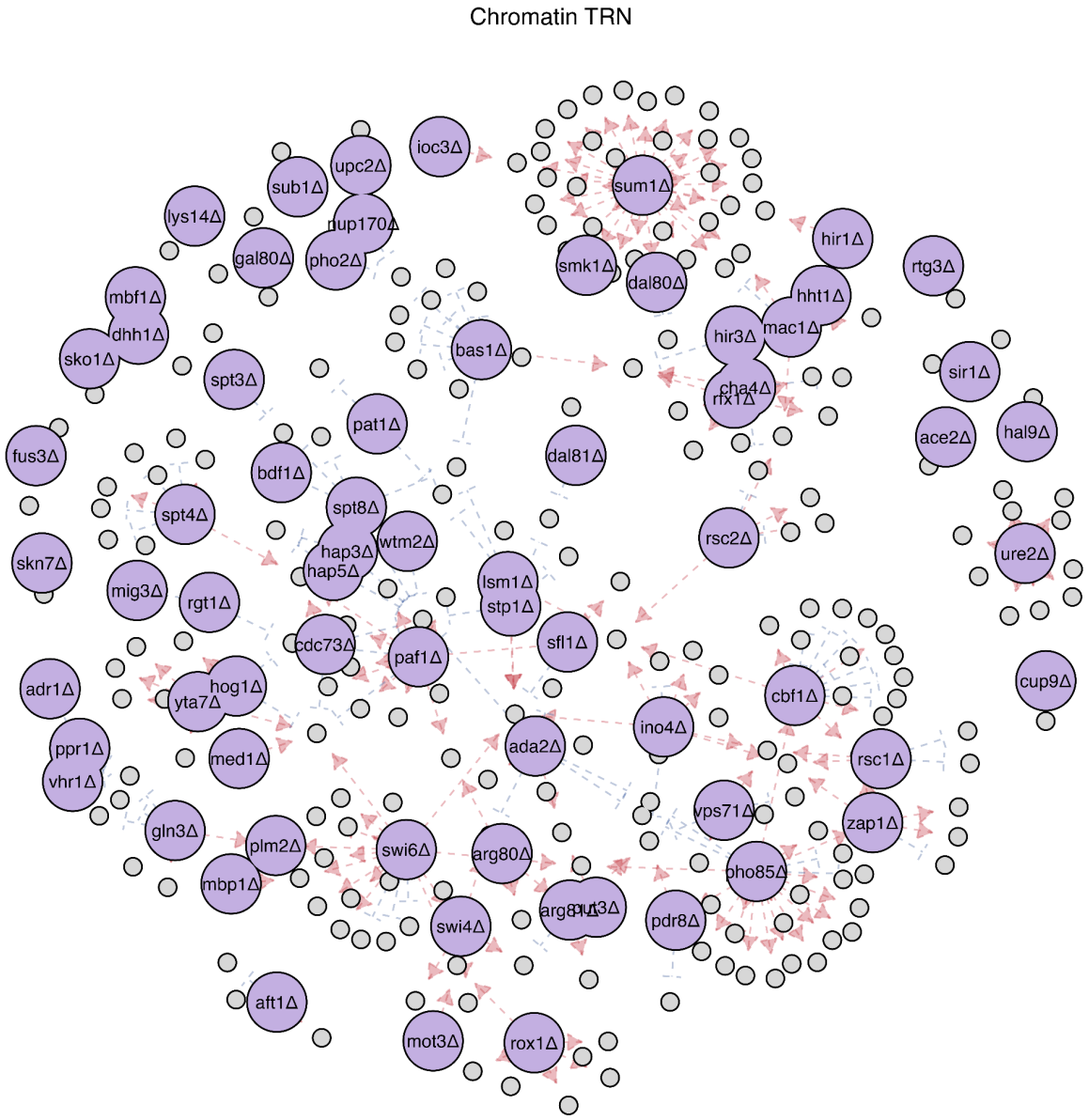

Supplemental Figure S14

Predicted regulatory network of all available mutants in the MNase-seq dataset. Edges are colored based on upregulation (red) or downregulation (blue) as predicted from chromatin features.

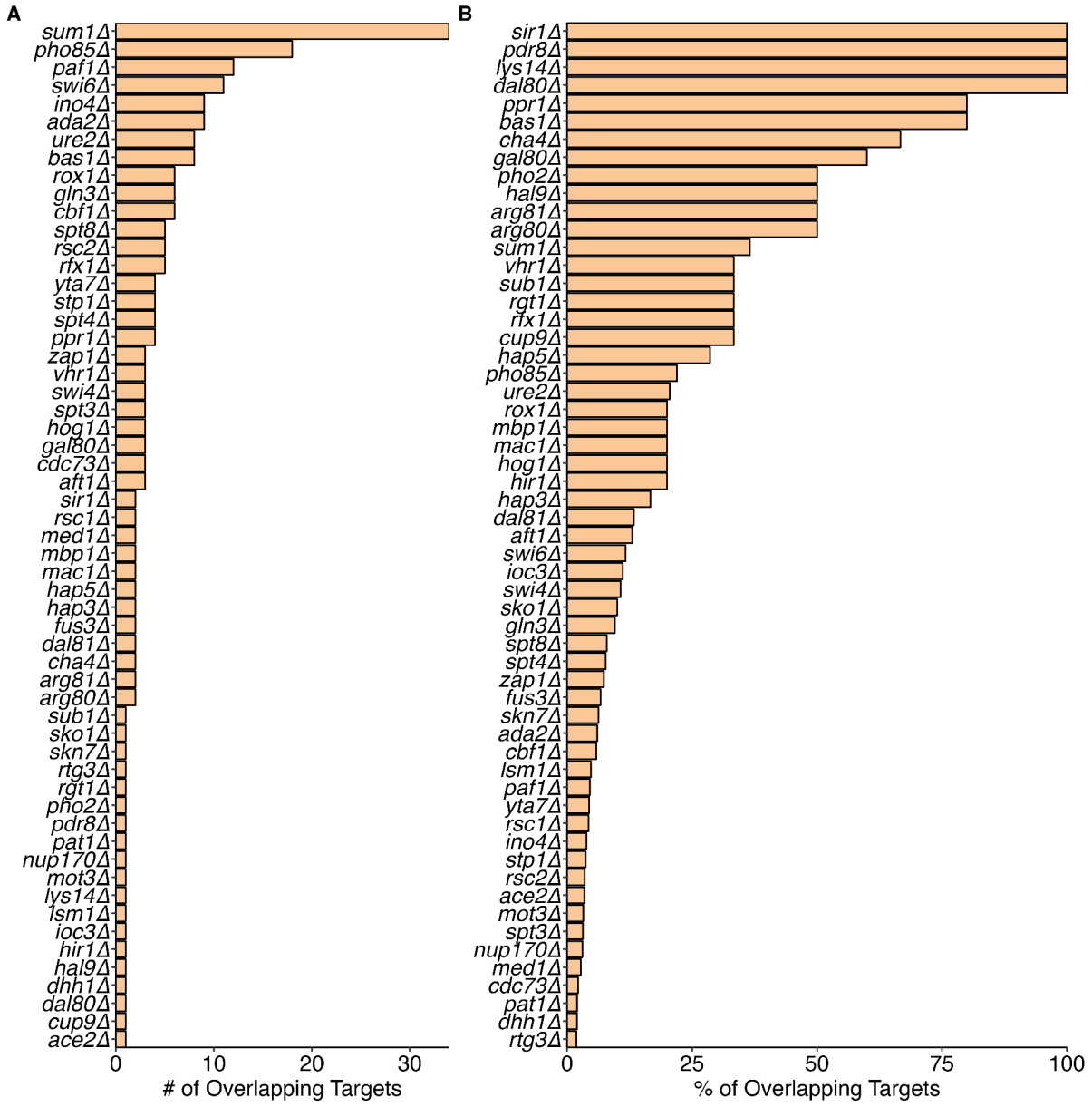

Supplemental Figure S15

Number of overlapping targets between an expression TRN and its corresponding chromatin TRN. Significant targets in the expression TRN were based on a $| \log_2(FC) | > 0.85$ cutoff and significant chromatin targets were based on the Laplacian cutoff. **(A)** Number of total overlapping targets. **(B)** Percent overlap of chromatin TRN vs. the expression TRN.

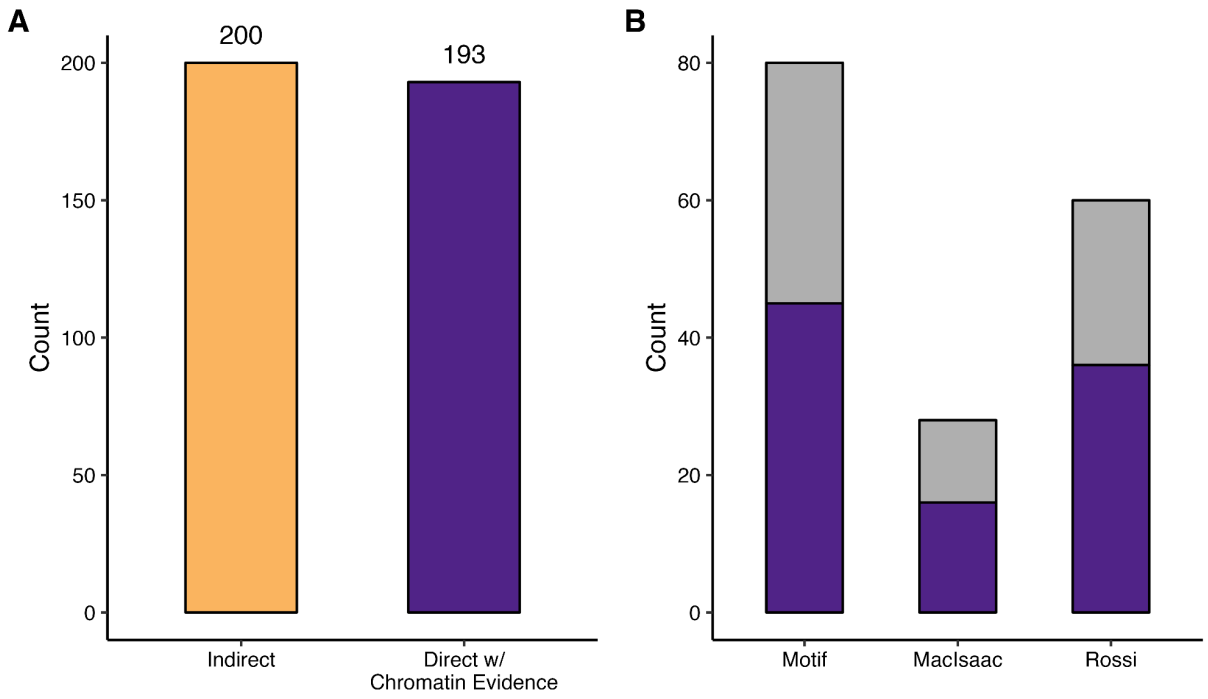

Supplemental Figure S16

Characterization of direct interactions using chromatin evidence. (A) Bar plot displaying the number of significant direct vs. indirect interactions in this dataset. Direct interactions (n = 178) are validated with both annotated binding site data and measured TF occupancy change. **(B)** Validation of annotated TF binding sites by motif (FIMO), MacIsaac et al., and Rossi et al. with measured TF occupancy changes. Purple represents binding sites or motifs exhibiting a significant TF occupancy change ($|\log_2(FC)| > 0.5$).